New Insights on the Origins of the Stereocontrol of the Staudinger Reaction: [2 + 2] Cycloaddition between Ketenes and *N*-Silylimines

Ana Arrieta and Fernando P. Cossío*

Kimika Fakultatea, Euskal Herriko Unibertsitatea, P.K. 1072, 20080 San Sebastián-Donostia, Spain

Begoña Lecea

Farmazi Fakultatea, Euskal Herriko Unibertsitatea, P.K. 450, 01080 Vitoria-Gasteiz, Spain

qopcomof@sc.ehu.es

Received May 22, 2000

Density-functional theory studies on the [2 + 2] reaction between *N*-silylimines and ketenes to form the corresponding 2-azetidinones (β-lactams) help to clarify several aspects on the mechanism of the Staudinger reaction. This reaction has been studied experimentally by Panunzio et al. It is shown that the formation of the 2-azetidinone ring takes place via two consecutive reactions. The first reaction consists of the nucleophilic addition of the iminic nitrogen to the sp-hybridized carbon atom of the ketene, with simultaneous migration of the silyl group from the imine to the oxygen atom of the ketene. This leads to silyl enol intermediates, in good agreement with the experimental results. Formation of the N-silylated β-lactam takes place via a domino reaction consisting of a conrotatory thermal electrocyclization followed by a new silatropic rearrangement. It is also found that isomerization of the starting *N*-silylimine has a lower activation barrier than that associated with the formation of the C−N bond, which explains the stereochemical outcome experimentally observed. Further considerations on the asymmetric torquoelectronic effects involved in this reaction are also reported.

Introduction

The Staudinger reaction[1] between ketenes and imines is one of the most convenient forms to obtain 2-azetidinones (β-lactams) in a convergent and stereocontrolled manner.[2] The importance of this reaction stems from the utility of β-lactams in medicinal chemistry[3] and from the utility of the obtained cycloadducts in the synthesis of compounds of biological interest.[4] In addition, the reaction is very versatile and therefore can be used in combinatorial chemistry.[5] Given the importance of this reaction, several experimental[6] and computational[7,8] studies have been reported to understand its mechanism, with particular emphasis on the origins of its stereocontrol. From these studies, it is now commonly accepted that the reaction is stepwise in nature, instead of a concerted (although asynchronous) [2 + 2] cycloaddition. The first step of the reaction consists of a nucleophilic attack of the iminic nitrogen to the sp-hybridized carbon atom of the ketene to form a zwitterionic intermediate. This intermediate is transformed into the reaction product via a conrotatory thermal electrocyclization (Scheme 1). This latter step is therefore subjected to torquoelectronic effects.[9]

Within this context, Panunzio et al.[10,11] have published recently several very interesting contributions on the Staudinger reaction between ketenes and *N*-silylimines (Scheme 2). Aside from the synthetic interest of these reactions, they provide new insights on the mechanism of this formal [2 + 2] cycloaddition.

Thus, the stepwise nature of the Staudinger reactions studied by Panunzio is evidenced by the isolation of the O-silylated intermediates shown in Scheme 2. Actually, the formation of *N*-silylazetidin-2-ones from ketenes and *N*-silylimines consists of two consecutive reactions.[12] The

---

[1] Staudinger, H. *Justus Liebigs Ann. Chem.* **1907**, *356*, 51.

[2] (a) Georg, G. I.; Ravikumar, V. T. In *The Organic Chemistry of β-Lactams*; Georg, G. I., Ed.; VCH Publishers: New York, 1993; pp 295−368. (b) Tidwell, T. T. *Ketenes*; Wiley: New York, 1995; pp 518−536. (c) Palomo, C.; Aizpurua, J. M.; Ganboa, I.; Oiarbide, M. *Eur. J. Org. Chem.* **1999**, *3223*, 3.

[3] (a) *Chemistry and Biology of β-Lactam Antibiotics*; Morin, R. B., Gorman, M., Eds.; Academic Press: New York, 1982; Vols 1−3. (b) van der Steen, F. H.; van Koten, G. *Tetrahedron* **1991**, *47*, 7503.

[4] (a) Manhas, M. S.; Wagle, D. R.; Chiang, J.; Bose, A. K. *Heterocycles* **1988**, *27*, 1755. (b) Ojima, I. *Acc. Chem. Res.* **1995**, *28*, 383.

[5] (a) Ruhland, B.; Bhandari, A.; Gordon, E. M.; Gallop, M. A. *J. Am. Chem. Soc.* **1996**, *118*, 253. (b) Molteni, V.; Annunziata, R.; Cinquini, M.; Cozzi, F.; Benaglia, M. *Tetrahedron Lett.* **1998**, *39*, 1257. (c) Annunziata, R.; Benaglia, M.; Cinquini, M.; Cozzi, F. *Chem. Eur. J.* **2000**, *6*, 133.

[6] (a) Lynch, J. E.; Riseman, S. M.; Laswell, W. L.; Tschaen, D. M.; Volante, R. P.; Smith, G. B.; Shinkay, I. *J. Org. Chem.* **1989**, *54*, 3792. (b) Hegedus, L. S.; Montgomery, J.; Narukawa, Y.; Snustad, D. C. *J. Am. Chem. Soc.* **1991**, *113*, 5784.

[7] (a) Cossío, F. P.; Ugalde, J. M.; Lopez, X.; Lecea, B.; Palomo, C. *J. Am. Chem. Soc.* **1993**, *115*, 995. (b) Cossío, F. P.; Arrieta, A.; Lecea, B.; Ugalde, J. M. *J. Am. Chem. Soc.* **1994**, *116*, 2085. (c) Lecea, B.; Arrastia, I.; Arrieta, A.; Roa, G.; Lopez, X.; Arriortua, M. I.; Ugalde, J. M.; Cossío, F. P. *J. Org. Chem.* **1996**, *61*, 3070. (d) Arrieta, A.; Lecea, B.; Cossío, F. P. *J. Org. Chem.* **1998**, *63*, 5869.

[8] (a) Lopez, R.; Sordo, T. L.; Sordo, J. A.; Gonzalez, J. *J. Org. Chem.* **1993**, *58*, 7036. (b) Truong, T. M. *J. Phys. Chem. B* **1998**, *102*, 7877.

[9] (a) Niwayama, S.; Kallel, E. A.; Spellmeyer, D. C.; Sheu, C.; Houk, K. N. *J. Org. Chem.* **1996**, *61*, 2813. (b) Dolbier, W. R., Jr.; Korionak, H.; Houk, K. N.; Sheu, C. *Acc. Chem. Res.* **1996**, *29*, 471.

[10] (a) Martelli, G.; Spunta, G.; Pannunzio, M. *Tetrahedron Lett.* **1998**, *39*, 6257. (b) Pannunzio, M.; Bacchi, S.; Campana, E.; Fiume, L.; Vicennati, P. *Tetrahedron Lett.* **1999**, *40*, 8495. (c) Bandini, E.; Favi, G.; Martelli, G.; Panunzio, M.; Piersanti, G. *Org. Lett.* **2000**, *2*, 1077.

[11] Bandini, E.; Martelli, G.; Spunta, G.; Bongini, A.; Pannunzio, M.; Piersanti, G. *Tetrahedron*: *Asymmetry* **1999**, *10*, 1445.

10.1021/jo0007736 CCC: $19.00

Scheme 1[a]

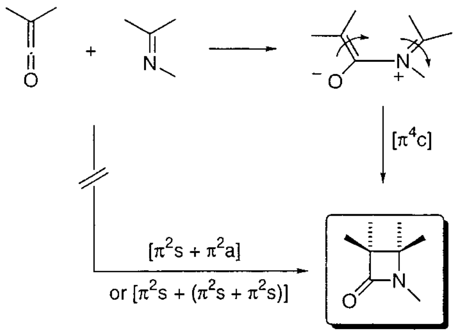

[a] The possible substituents at the different positions are not specified.

Scheme 2[a]

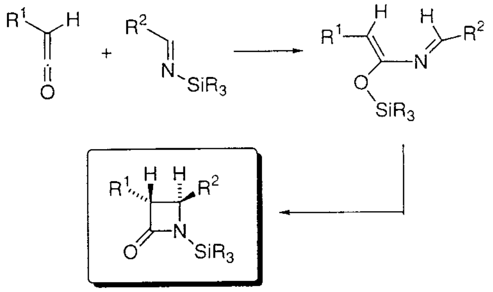

[a] In the chiral compounds only one enantiomer is drawn.

trans stereochemistry of the corresponding cycloadducts is what one should expect from the conrotatory electrocyclization of these intermediates. However, neither the structure nor the stereochemistry of the O-silylated intermediates reported by Panunzio is evident from the standard mechanism reported in Scheme 1. In addition, according to the standard model,[7,8a] cis-stereochemistry is predicted in the Staudinger reaction between ketenes and imines, instead of the trans cycloadducts reported by Panunzio. Moreover, this author has reported a very low stereoselection when chiral imines derived from enantiopure aldehydes are used.[10a,c] This result is not in agreement with the standard model.[7b]

Therefore, the aim of this paper is to study both the mechanism and the origins of the stereochemical outcome of the Staudinger reaction between *N*-silylimines and ketenes, to understand the anomalies observed experimentally and to introduce additional details in the commonly accepted general model for this reaction.

Computational Methods

All the calculations reported in this paper obtained with the GAUSSIAN 98 suite of programs,[13] using the 6-31G* basis set.[14] Electron correlation has been partially taken into account using the hybrid functional usually denoted as B3LYP.[15] Zero-point vibrational energy (ZPVE) corrections have been computed at the B3LYP/6-31G* level and have not been corrected. All stationary points have been characterized by harmonic analysis.[16] Several reaction paths have been checked by intrinsic reaction coordinate (IRC) calculations.[17] Donor–acceptor interactions and atomic charges[18] have been computed using the Natural Population Analysis (NPA).[19] The energies associated with these two-electron interactions have been

Scheme 3[a]

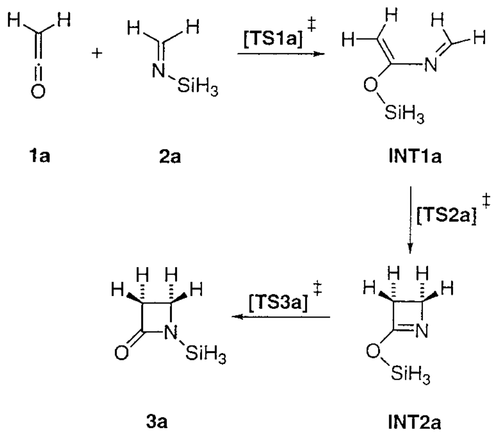

[a] In the chiral compounds only one enantiomer is drawn.

computed according to the following equation

$$\Delta E^{(2)}_{\phi\phi^*} = -n_\phi \frac{\langle \phi^* | \hat{F} | \phi \rangle^2}{\epsilon_{\phi^*} - \epsilon_\phi} \qquad (1)$$

where $\hat{F}$ is the DFT equivalent of the Fock operator and ϕ and ϕ^* are two filled and unfilled Natural bond orbitals having ϵ_ϕ and ϵ_{ϕ^*} energies, respectively. n_ϕ Stands for the occupation number of the filled orbital.[20] Hardnesses (η)[21] have been calculated by means of the following approximate expression

$$\eta = \frac{1}{2}(\epsilon_L - \epsilon_H) \qquad (2)$$

where ϵ_H and ϵ_L are the orbital energies of the HOMO and LUMO, respectively.

Results and Discussion

We have first studied the **1a** + **2a** → **3a**, which is the simplest example of this reaction. The reactants and products are reported in Scheme 3, together with the corresponding reaction intermediates found in the B3LYP/6-31G* potential energy surface.

The chief geometric and energetic features of the first step of this reaction are reported in Figure 1. The first

---

(12) For the definition of consecutive and domino (tandem) reactions, see Tietze, L. F.; Beilfuss, V. *Angew. Chem., Int. Ed. Engl.* **1993**, *32*, 131.

(13) Gaussian 98, Revision A.5: Frisch, M. J.; Trucks, G. W.; Schlegel, H. B.; Scuseria, G. E.; Robb, M. A.; Cheeseman, J. R.; Zakrzewski, V. G.; Montgomery, J. A., Jr.;. Stratmann, R. E.; Burant, J. C.; Dapprich, S.; Millam, J. M.; Daniels, A. D.; Kudin, K. N.; Strain, M. C.; Farkas, O.; Tomasi, J.; Barone, V.; Cossi, M.; Cammi, R.;. Mennucci, B.; Pomelli, C.; Adamo, C.; Clifford, S.; Ochterski, J.; Petersson, G. A.; Ayala, P. Y.;. Cui, Q.; Morokuma, K.; Malick, D. K.; Rabuck, A. D.; Raghavachari, K.; Foresman, J. B.; Cioslowski, J.; Ortiz, J. V.; Stefanov, B. B.; Liu, G.; Liashenko, A.; Piskorz, P.; Komaromi, I.; Gomperts, R.; Martin, R. L.; Fox, D. J.; Keith, T.; Al-Laham, M. A.; Peng, C. Y.; Nanayakkara, A.; Gonzalez, C.; Challacombe, M.; Gill, P. M. W.; Johnson, B.; Chen, W.; Wong, M. W.; Andres, J. L.; Gonzalez, C.; Head-Gordon, M.; Replogle, E. S.; Pople, J. A. Gaussian, Inc., Pittsburgh, PA, 1998.

(14) Hehre, W. J.; Radom, L.; Schleyer, P.v. R.; Pople, J. A. *Ab Initio Molecular Orbital Theory*; Wiley: New York, 1986; pp 65–88 and references therein.

(15) (a) Becke, A. D. *J. Chem. Phys.* **1993**, *98*, 5648. (b) Becke, A. D. *Phys. Rev. A* **1988**, *38*, 3098. (c) Lee, C.; Yang, W.; Parr, R. G. *Phys. Rev. B* **1980**, *37*, 785. (d) Vosko, S. H.; Wilk, L.; Nusair, M. *Can. J. Phys.* **1980**, *58*, 1200.

(16) McIver, J. W.; Komornicki, A. K. *J. Am. Chem. Soc.* **1972**, *94*, 2625.

(17) (a) Fukui, K. *Acc. Chem. Res.* **1981**, *14*, 363. (b) Gonzalez, C.; Schlegel, H. B. *J. Chem. Phys.* **1989**, *90*, 2154. (c) Gonzalez, C.; Schlegel, H. B. *J. Phys. Chem.* **1990**, *94*, 5523.

(18) Wiberg, K. B.; Rabien, P. R. *J. Comput. Chem.* **1993**, *14*, 1504.

(19) Reed, A. E.; Curtiss, L. A.; Weinhold, F. *Chem. Rev.* **1988**, *88*, 899.

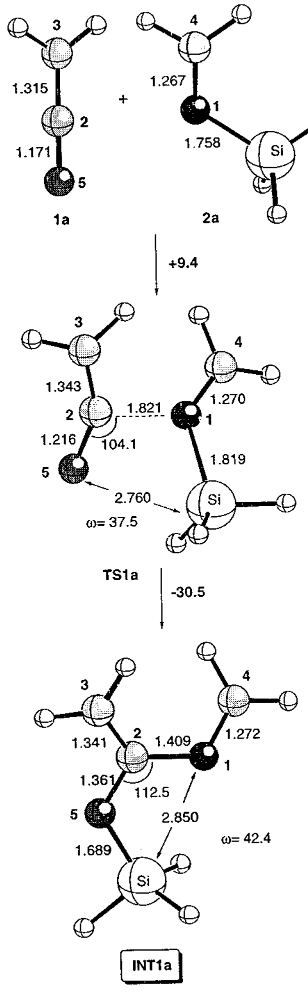

Figure 1. B3LYP/6-31G* main geometric and energetic features computed for the formation of the N1−C2 bond in the **1a** + **2a** → **3a** transformation. Bond distances and angles are given in Å and deg, respectively. The bold numbers above the arrows are the differences in energy computed at the B3LYP/6-31G*+ΔZPVE level.*ω* is the N1−C2−C3−C4 dihedral angle. Unless otherwise stated, the atoms are represented by increasing order of shading as follows: H, C, O, N.

transition structure **TS1a**, which lies 9.4 kcal/mol above the separate reagents, is found to be quite similar to that found for the Staudinger reaction between ketene and methanimine,[7,8] the main difference being the low value of the *ω* dihedral angle, defined as N1−C2−C3−C4 (see Figure 1). Thus, our calculations show an almost synperiplanar relationship between C3 and C4, whereas in the Staudinger reaction between ketene and methanimine the computed conformation is antiperiplanar.[7,8] This different value for the dihedral angle stems from the two-electron stabilizing interaction between one lone pair of the oxygen atom and one antibonding Si−H localized *σ** orbital, according to the NPA of **TS1a**:

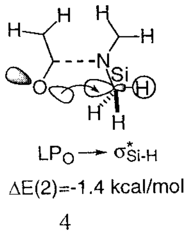

4

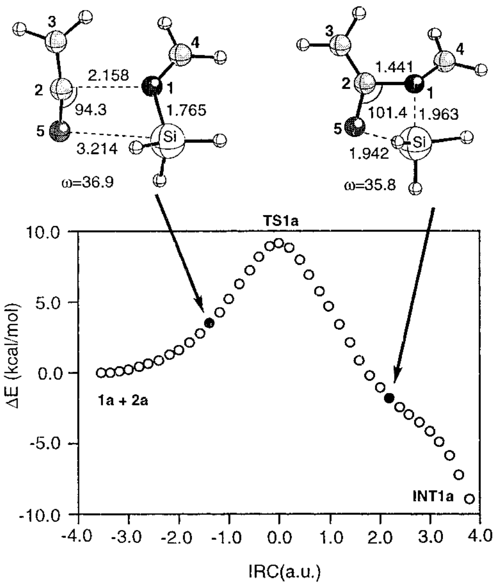

Figure 2. B3LYP/6-31G* IRC plot associated with the first step of the **1a** + **2a** → **3a** reaction, showing that both the formation of the N1−C2 bond and the 1,3-sylatropic rearrangement from N1 to O5 take place via **TS1a**.

It is also noteworthy that in **TS1a** the N1−Si bond distance is slightly larger than in **2a** (Figure 1). Actually, our calculations show that aside from the formation of the N1−C2 bond, a silatropic rearrangement from N1 to O5 takes place. Thus, the product formed after the first step of the reaction is the neutral silyl enol ether **INT1a**, instead of the zwitterionic intermediate depicted in Scheme 1. We have performed an IRC calculation to verify that **TS1a** connects **INT1a** with the reactants. The corresponding profile is shown in Figure 2. In this Figure we have selected two "halfway" points between the saddle point and the corresponding local minima. The geometries of these points clearly show that formation of the N1−C2 bond is faster than the migration of the silyl group. Thus, as long as the N1−C2 bond is formed the negative charge on O5 increases thus facilitating the formation of the O5−Si bond. The Si−O bond is more stable than the Si−N bond. For instance, in the following isogyric equation

$$\mathrm{HOSiH_3} + \mathrm{NH_3} \xrightarrow{\Delta E} \mathrm{H_2NSiH_3} + \mathrm{H_2O}$$

we have found that $\Delta E = +11.8$ kcal/mol at the B3LYP/6-31G*+ΔZPVE level.[22] Therefore, given the high oxophilicity of silicon and the neutral character of **INT1a**, this latter stationary point lies ca. 21 kcal/mol below the separate reactants.

From **INT1a**, the next step consists of the formation of the C3−C4 bond via **TS2a**. The harmonic analysis shows that this latter transition structure corresponds to a conrotatory electrocyclization, with a concomitant

---

(20) For several recent papers including combined B3LYP and NPA see: (a) Glendening, E. D.; Hrabal, J. A. *J. Am. Chem. Soc.* **1997**, *119*, 12940. (b) Krapp, J.; Remko, M.; Schleyer, P.v. R. *Inorg. Chem.* **1997**, *36*, 4241. (c) García, A.; Cruz, E. M.; Sarasola, C.; Ugalde, J. M. *J. Phys. Chem. A* **1997**, *101*, 3021. See also ref 7d.

(21) (a) Parr, R. G.; Donnelly, R. A.; Levy, M.; Palke, W. E. *J. Chem. Phys.* **1978**, *68*, 3801. (b) Parr, R. G.; Pearson, R. G. *J. Am. Chem. Soc.* **1983**, *105*, 7512. (c) Mulliken, R. S. *J. Chem. Phys.* **1934**, *2*, 782.

(22) The total energies (in au) at the B3LYP/6-31G* level + ΔZPVE of the silylated species are the following: $\mathrm{HOSiH_3}$, −367.10430; $\mathrm{H_2NSiH_3}$, −347.21109.

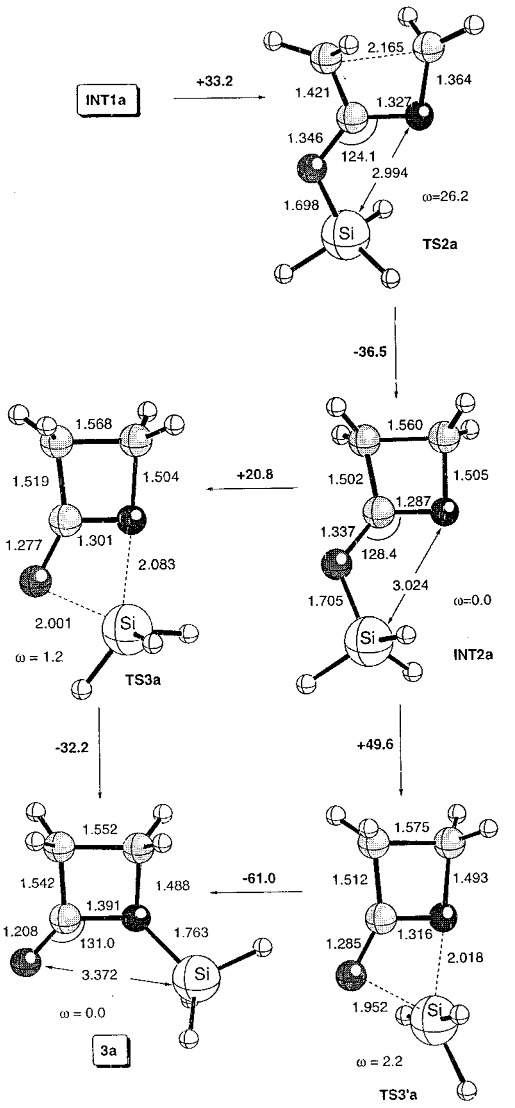

Figure 3. B3LYP/6-31G* main geometric and energetic features found for the formation of **3a** from the O-silylated intermediate **INT1a**. See Figure 1 caption for additional details.

formation of an additional π-bond between N1 and C2. The main features of this second saddle point are shown in Figure 3. The activation barrier for this second step is calculated to be ca. 33 kcal/mol, which is significantly larger than those calculated for standard Staudinger reactions.[7,8] Therefore, from the energetic point of view, **INT1a** lies in a considerably deep well. This explains why this kind of intermediate has been isolated and characterized by Panunzio et al.,[10,11] instead of the corresponding four-membered cycloadducts. The reasons for these relatively large activation barriers are the oxophilicity of silicon and the generation of an endocyclic double bond during the step leading to the formation of **INT2a**.

The next step of the reaction is the formation of **3a** from **INT2a**. According to our calculations, **3a** is 11.4 kcal/mol more stable than the corresponding silyl enol ether (Figure 3). In this case, the lower N−Si bond energy with respect to the Si−O bond is compensated by the strain relief on passing from the endocyclic C=N bond to the corresponding amide.

We have found two transition structures connecting **INT2a** with **3a**, and their chief features are collected in Figure 3. In the first one, denoted as **TS3a**, there is a retention of configuration at the silicon atom. In contrast, in the second case, denoted as **TS3′a**, the silatropic rearrangement takes place with inversion of configuration at silicon. According to our results, **TS3′a** is ca. 29 kcal higher in energy than **TS3a**. Therefore, although no experiments using chiral silyl atoms have been performed, our results predict that formation of N-silylated cycloadducts must take place with retention of configuration. Inspection of the MOs of **TS3a** and **TS3′a** shows that this step does not consist of a 1,3-sigmatropic reaction[23] but of a nucleophilic attack of the nitrogen on the silyl group, the oxygen atom acting as a leaving group, as depicted in Scheme 4.

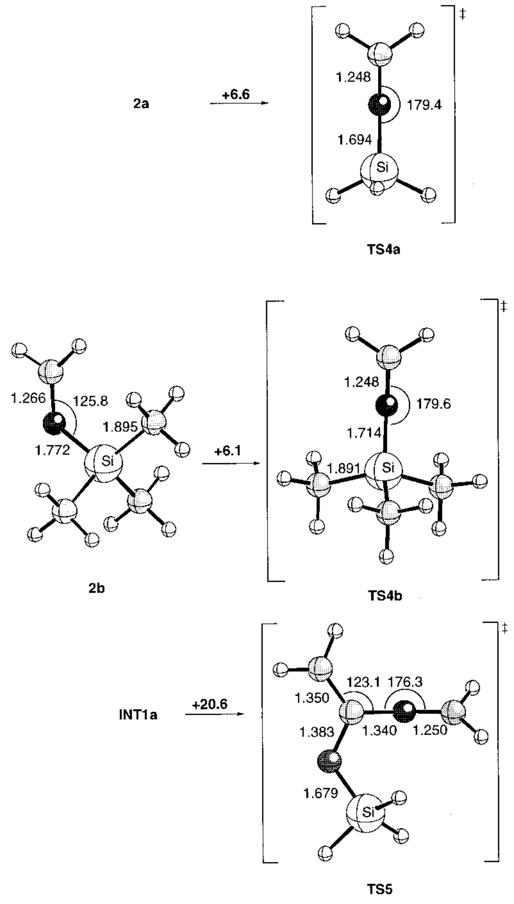

Figure 4. B3LYP/6-31G* main geometric and energetic features of the transition structures associated with isomerization of imines **1a,b** and **INT1a**. See Figure 1 caption for additional details.

Finally, our calculations predict that the activation energy corresponding to the silatropic rearrangement is ca. 16 kcal/mol lower than that associated with the electrocyclic step (see Figure 3). Therefore, it is expected that cycloadducts **3a** should be isolated, in agreement with the experimental observations of Panunzio et al.[10]

There is another intriguing feature of this reaction, namely the exclusive isolation of (*Z,E*)-silyl enol ethers and therefore *trans*-*N*-silyl-2-azetidinones. If one imine interacts with an unsymmetrically substituted ketene, two kinds of attacks of the imine lone pair on the sp-hybridized carbon atom of the ketene can be envisaged,

---

[23] Woodward, R. B.; Hoffmann, R. *The Conservation of Orbital Symmetry*; Academic Press: New York, 1970; pp 114−140.

Scheme 4

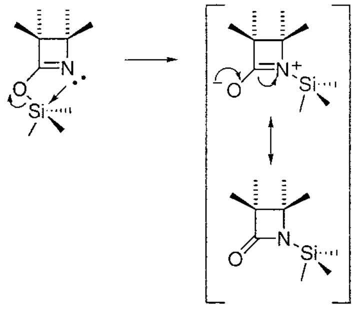

Scheme 5

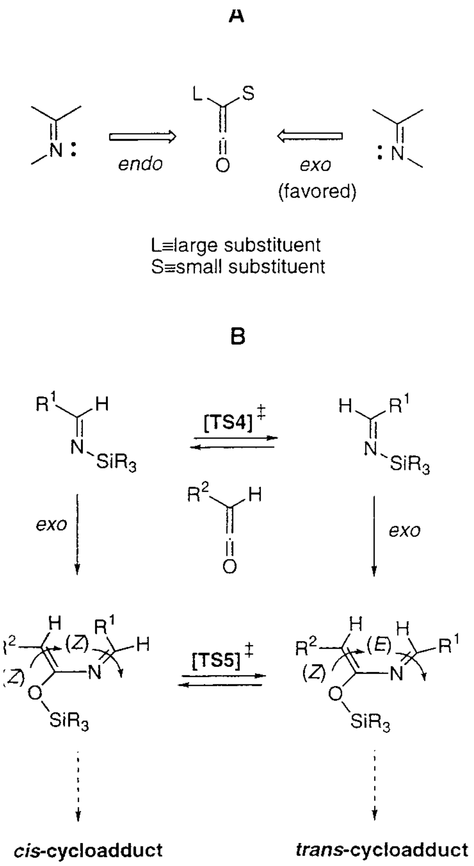

as depicted in Scheme 5A. Previous studies from our group have shown[7] that the exo attack of a (*E*)-imine leads to the precursor of the corresponding cis-cycloadduct (Scheme 5B). Alternatively, the isomeric (*Z*)-imine must yield in the end the experimentally observed *trans*-2-azetidinone. Since only the precursors of the trans isomers have been observed by Panunzio et al.,[10a] this implies isomerization around the C=N bond in the starting imines or in the iminic part of the intermediate silyl enol ethers (Scheme 5B).

To test this hypothesis, the topomerization of imines **2a,b** was studied, and the corresponding transition structures **TS4a,b** are reported in Figure 4. As it can be seen, the activation energies are of ca. 6 kcal/mol, a value smaller than those found in *N*-alkyl or *N*-arylimines.[24] The corresponding imaginary frequencies are associated with the distortion of the C−N−Si angle, thus indicating that the topomerization consists of an inversion of the nitrogen atom instead of a rotation around the C=N bond.[24] The almost linear structure of **TS4a,b** is stabilized by a donation from the lone pair of the nitrogen to one d-orbital of silicon and to the $\sigma^*_{\mathrm{Si-R}}$ orbitals, R being hydrogen or methyl:

Scheme 6

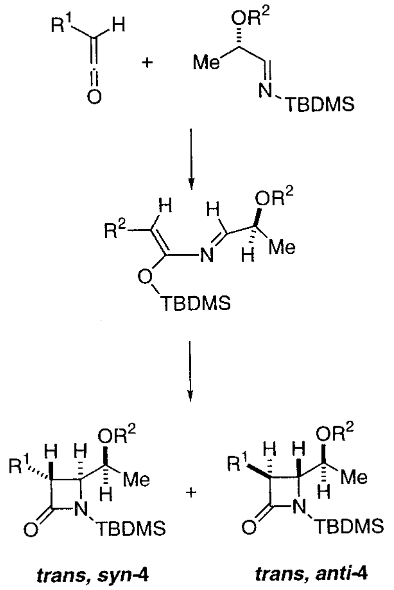

(d.e.= 0-20%)

R1=phtalimidoyl, halogen
R2=methyl, benzyl, trialkylsilyl

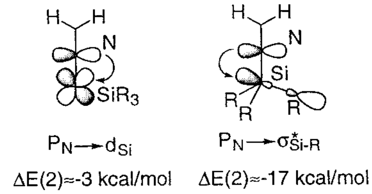

In contrast, these stabilizing interactions are not present in the case of **TS5**, and as a consequence the activation energy associated with the topoisomerization of **INT1a** is much larger (see Figure 4). In summary, preferential formation of intermediates depicted in Scheme 5 must take place via previous isomerization of the starting *N*-silylimine followed by an exo attack over the monosubstituted ketene.

Another remarkable feature of this reaction is that its diastereocontrol is much lower than that usually observed in the standard Staudinger reaction. For example, almost negligible diastereocontrol is observed when *N*-silylimines derived from lactalaldehydes react with phtahlimidoyl ketene (Scheme 6).[10a] This result is in sharp contrast with more conventional Staudinger reactions, since in these cases only one cis-stereoisomer is obtained, with complete stereocontrol (Scheme 7).[2a,7b]

To investigate the origin of these different results and given that the conrotatory step leading to the formation of the C3−C4 bond determines the stereochemical outcome of the reaction, we studied the features of the transition structures shown in Figures 5 and 6. The corresponding relative energies and other relevant magnitudes are reported in Table 1.

---

[24] Eliel, E. L.; Wilen, S. H.; Mander, L. N. *Stereochemistry of Organic Compounds*; Wiley: New York, 1994; pp 550−555, and references therein.

Scheme 7

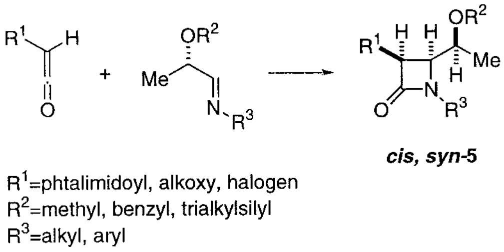

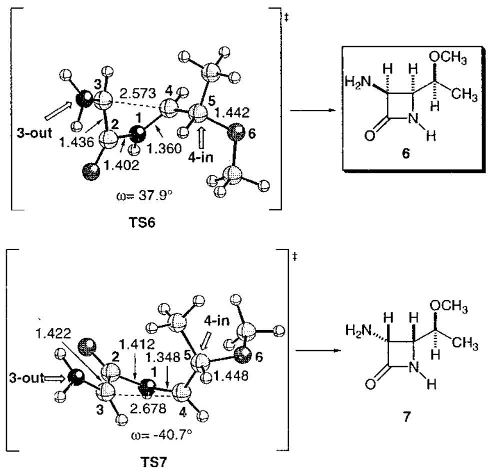

Figure 5. B3LYP/6-31G* main geometric features computed for saddle points **TS6** and **TS7**, leading to cis,syn and cis,anti cycloadducts **6** and **7**, respectively. See Figure 1 caption for additional details.

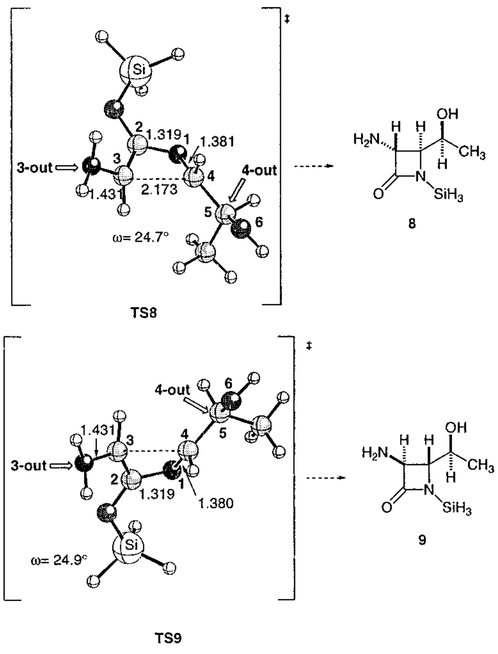

Figure 6. B3LYP/6-31G* main geometric features computed for saddle points **TS8** and **TS9**, leading to trans,syn and trans,-anti cycloadducts **8** and **9**, respectively. See Figure 1 caption for additional details.

We have computed saddle points **TS6** and **TS7** leading to cis,syn and cis,anti cycloadducts **6** and **7**, respectively (Figure 5). These structures incorporate the main features of the reactions studied experimentally (see Scheme 6). Since in these cases the (*E*)-imines do not isomerize, the exo attack leads to two alternative transition structures in which the substituents at C3 and C4 occupy the 3-out and 4-in positions, respectively. The in and out terms refer to the inward and outward terms used by Houk in his treatment of torquoelectronic effects in conrotatory reactions involving cyclobutenes.[9] According to our results, **TS6** is ca. 5 kcal/mol more stable than **TS7** (Table 1). This considerable energy difference implies exclusive formation of the cis,syn cycloadduct **6** in perfect agreement with the experimental results.[2a,7b]

Table 1. [a] **Relative Energies**[b] **(ΔE_{Rel}, kcal/mol), Hardnesses**[c]**(η, kcal/mol), and Wiberg Bond Indices**[d] **between C3 and C4 Atoms ($B_{3,4}$, au) of Transition Structures TS6-ts8**

structure	ΔE_{rel}	η	$B_{3,4}$
TS6	0.0	33.0	0.321
TS7	+4.7	30.0	0.280
TS8	0.0	54.6	0.480
TS9	+0.1	54.1	0.478

[a] All magnitudes have been computed at the B3LYP/6-31G* level on previously optimized structures (see Figures 5 and 6). [b] Zero-point energy corrections have been included. [c] Computed by means of eq 2. [d] Computed by means of the natural bonding analysis.

Second-order perturbation theory reveals the origins of this stereocontrol. In both saddle points there is a two-electron donation from the $\sigma_{3,4}$ localized orbital to $\sigma^*_{5,6}$. This implies an almost linear arrangement between the C3, C5 and O6 atoms (see Figure 5). However, in **TS7** the disposition of the methyl group generates a considerable steric congestion which in turn promotes a larger C3···C4 bond distance and consequently a lower bond order between both atoms (see Figure 5 and Table 1). Therefore, the overlap between the donor and acceptor localized orbitals in **TS7** is considerably lower than in **TS6**:

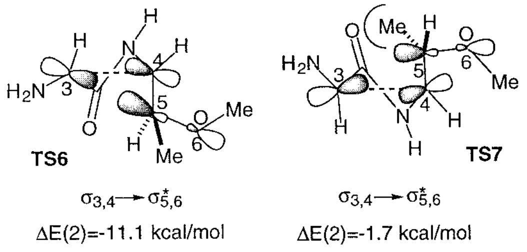

The final result is that **TS6** is of lower energy and harder[25] (see Table 1) than **TS7**.

We have also studied transition structures **TS8** and **TS9** depicted in Figure 6. In this case, the isomerization of the starting imines and subsequent exo attack lead to transition structures in which both substituents at C3 and C4 are in an out disposition with respect to the four-membered rings being formed (Figure 6). This outward disposition of the chiral group leads to a negligible torquoelectronic effect. Thus, the two-electron interactions reported above are of only ca. −2 kcal/mol and very similar in both cases. As a consequence, both **TS8** and **TS9** are of similar energy and hardness (see Table 1),

---

(25) For recent related studies on the relationship between DFT-based HSAB descriptors and regio- and stereoselectivity in thermal cycloadditions see: (a) Daumon, S.; Van de Woude, G.; Méndez, F.; Geerlings, P. *J. Phys. Chem. A* **1997**, *101*, 886. (b) Chandra, A. K.; Nguyen, M. T. *J. Phys. Chem. A* **1998**, *102*, 6181. (c) Méndez, F.; Tamariz, J.; Geerlings, P. *J. Phys. Chem. A* **1998**, *102*, 6292. (d) Nguyen, L. T.; Le, T. N.; De Proft, F.; Chandra, A. K.; Langenaeker, W.; Nguyen, M. T.; Geerlings, P. *J. Am. Chem. Soc.* **1999**, *121*, 5992.

and a negligible stereoselection between the two possible trans cycloadducts is predicted, in good agreement with the experimental results.

Conclusions

Our computational study on the reaction between ketenes and N-silylated imines leads to the following conclusions:

(i) The formation of the *N*-silyl-2-azetidinones takes place via two consecutive[12] reactions. The first reaction consists of a nucleophilic attack of the iminic nitrogen on the sp-hybridized carbon atom of the ketene, with a concomitant migration of the silyl group from the nitrogen to the oxygen atom. The second reaction is a domino[12] process involving a conrotatory electrocyclization leading to the ring closure, followed by a new migration of the silyl group yielding the experimentally observed N-silylated β-lactam. Both silatropies are predicted to occur with retention of configuration at the silicon atom and do not involve sigmatropic shifts.

(ii) The isomerization of the N-silylated imines has lower activation energy than the bond-forming steps, thus indicating that these isomerizations via inversion at the nitrogen are involved in the observed trans stereoselectivity.

(iii) The torquoelectronic effects present in the conrotatory step are very efficient when the chiral group is *inward* with respect to the ring being formed, thus leading to virtually perfect stereocontrol in the corresponding cis cycloadducts. In contrast, this stereocontrol is much lower or negligible when these chiral groups are *outward*, thus yielding mixtures of the possible trans cycloadducts.

In summary, the results reported for the variant of the Staudinger reaction[26] developed by Panunzio et al. confirm the validity of the previously reported model, namely the stepwise nature of the mechanism and the importance of torquoelectronic effects.

Acknowledgment. This work has been supported by the Gobierno Vasco-Eusko Jaurlaritza (Projects EX-1998-126 and PI-1998-116 and Fondo de Cooperación Aquitania/Euskadi) and by the Provintial Government of Gipuzkoa (Gipuzkoako Foru Aldundia).

Supporting Information Available: Tables including the total energies (hartree), the zero-point vibrational energies (hartree/particle), and the Cartesian coordinates (Å) of all the stationary points discussed in the text. This material is available free of charge via the Internet at http://pubs.acs.org.

JO0007736

---

(26) After the submission of this work, Bongini, Pannunzio et al. have reported ab initio calculations (MP2, QCISP(T) levels) on the **1a** + **2a** → **3a** transformation. At these levels of theory, the main results obtained by these authors are in agreement with those reported in the first part of our paper. See: Bongini, A.; Panunzio, M.; Piersanti, G.; Bandini, E.; Martelli, G.; Spunta, G.; Venturini, A. *Eur. J. Org. Chem.* **2000**, 2379.